

Structural, Optical and Thermal Characterization of PVA/2HEC Polyblend Films

G. Attia¹ and M.F.H. Abd El-kader^{2,*}

¹ Department of physics, Faculty of Science, El-Fayoum University, El-Fayoum, Egypt.

² Department of biophysics, Faculty of Science, Cairo University, Giza, Egypt.

*E-mail: mfhamed@hotmail.com

Received: 17 February 2013 / *Accepted:* 11 March 2013 / *Published:* 1 April 2013

Blends of two biodegradable polymer, polyvinyl alcohol (PVA) and 2-hydroxy ethyl cellulose (2HEC) were prepared with different compositions by using cast technique. X-ray diffraction (XRD) scans revealed the semi-crystalline nature of the blends for low concentration of 2HEC up to 50 wt% and the amorphous nature for higher ones. Infrared spectra (IR) of blend samples indicate that there is a compatibility between PVA and 2HEC through the formation of hydrogen-bonding between their polar groups. The absorption coefficient spectral analysis revealed the existence of long and wide band tails of the localized states. The absorption edge and band tails were estimated for pure and blend films from their optical absorption spectra. The thermal stability and thermal behavior of blends were investigated under non-isothermal conditions by thermogravimetry (TG) and differential thermal analyses (DTA). A single glass transition temperature for each blend was observed, which supports the existence of compatibility of such system. The kinetic parameters such as activation energy, entropy, enthalpy and Gibbs energy based on TG data for all samples in first decomposition region were determined using Coats-Redfern relation.

Keywords: XRD, IR spectra, UV/visible spectra, thermal parameters.

1. INTRODUCTION

Polymer blends formed with homo-or-copolymer are of a great importance because they allow the optimization of certain properties compared with isolated polymers [1-4]. Polymeric composite materials, both of natural and synthetic origin, constitute by far the broadest and most diverse class of biomaterials.

PVA is an efficient binder for solid pigments, ceramic products, plastic, cement, fibers, non-woven fabrics, catalyst pellets, cork compositions etc. Also, PVA has gained increasing attention in the

biomedical field due to its bioinertness [5-10]. The non-ionic polymer 2HEC is used in personal care applications, as its use in hair shampoo to satisfy many functions. Also, it's used to thicken shampoo, reduce foaming and enhance cleaning capability by forming collides around dirt particles [11] as well as viscosity modification in paints and cosmetics [12]. Blending PVA with other polymers may offer opportunities to modify the physical properties, improve the processability and lower the cost [13]. Both PVA and 2HEC possesses a film-forming property. Accordingly, PVA/2HEC film was thought to be a good candidate to improve the cost-performance ratio on commercial products and of significant practical applications.

Analysis of the absorption spectra in the lower energy part gives information about atomic vibrations, while the higher energy part of the spectrum gives a knowledge about electronic state in the atoms. The thermogravimetry analysis and differential thermal analyses curves provide some information about the various unexpected observations during heat treatment. The combination of these experimental techniques allows us to gain more complete understanding of the effect of composition on the structure and thermal stability of blend system.

In the present work the structural, optical and thermal properties of PVA/2HEC blends in the range of compositions 30-70 wt% PVA were investigated. In addition, the thermodynamic and optical parameters are discussed.

2. EXPERIMENTAL DETAILS

Poly (vinyl alcohol) with M_w of 20,000 and minimum degree of hydrolysis of 87% was purchased from BDH limited (Poole, England). 2-hydroxyethyle cellulose with M_w of 300,000 and viscosity is 80-125 mpa.s was supplied by Sigma-Aldrich Company, USA.

Weighed amounts of both PVA and 2HEC were dissolved separately in a mixture of distilled water and ethanol with ratio 4:1 at room temperature. A solution of PVA and 2HEC were mixed together with different weight percentages of PVA/2HEC (100/0, 70/30, 50/50, 30/70 and 0/100 wt/wt%) using a magnetic stirrer at 50 °C. Thin films of appropriate thickness (≈ 0.1 mm) were cast onto stainless steel Petri dishes and then dried in a furnace at 75 °C until the solvent was completely evaporated.

X-ray diffraction patterns were obtained using DIANO corporation, USA equipped with Cu K_α radiation ($\lambda=1.540 \text{ \AA}$, the tube operated at 30 kV, the Bragg angle (2θ) in the range 5-60°). FTIR measurements were carried out using the single beam Fourier transform infrared spectrophotometer (FT-IR-430, JASCO, Japan). FTIR spectra of the samples were obtained in the spectral range of 4000-400 cm^{-1} . Ultra violet and visible (UV/VIS) absorption spectra were measured using spectrophotometer (V-570 UV/VIS/NIR, JASCO, Japan). The differential thermal analysis of the prepared films was carried out using an equipment type (DTA-50 Schimoduzu corporation, Kyoto, Japan) from room temperature up to 400 °C with a heating rate of 10 °C/min. Perkin-Elmer (US, Norwalk, CT) TGA-7 was used for the thermogravimetric analysis of the samples. A small amount (5-10 mg) of the sample was taken for the analysis and the samples were heated from room temperature up to 400 °C at a rate of 10 °C/min. in nitrogen atmosphere.

3. RESULTS AND DISCUSSION

3.1. X-ray diffraction

Fig. 1 shows the x-ray diffraction of PVA and 2HEC homopolymers as well as their blend samples at room temperature in the scanning range $6^\circ \leq 2\theta \leq 60^\circ$. Spectrum (a) of pure PVA shows an intense reflection peak at $2\theta = 19.7^\circ$ diffused in the hallow amorphous region and was assigned to a mixture of (101) and (10 $\bar{1}$) reflections [14]. The appearance of sharp reflections and diffuse scattering is characteristic of crystalline and amorphous phases of conventional semi-crystalline polymers. However, spectrum (e) of pure 2HEC shows a broad amorphous halo with a scattered intensity maximum corresponding to $2\theta = 22^\circ$. It reflects the absence of any diffraction lines indicating the amorphous nature of 2HEC cast film. It is known that glassy amorphous polymers are typically optically clear, they show a liquid-like x-ray pattern [15]. This is consistent with the result of the 2HEC sample.

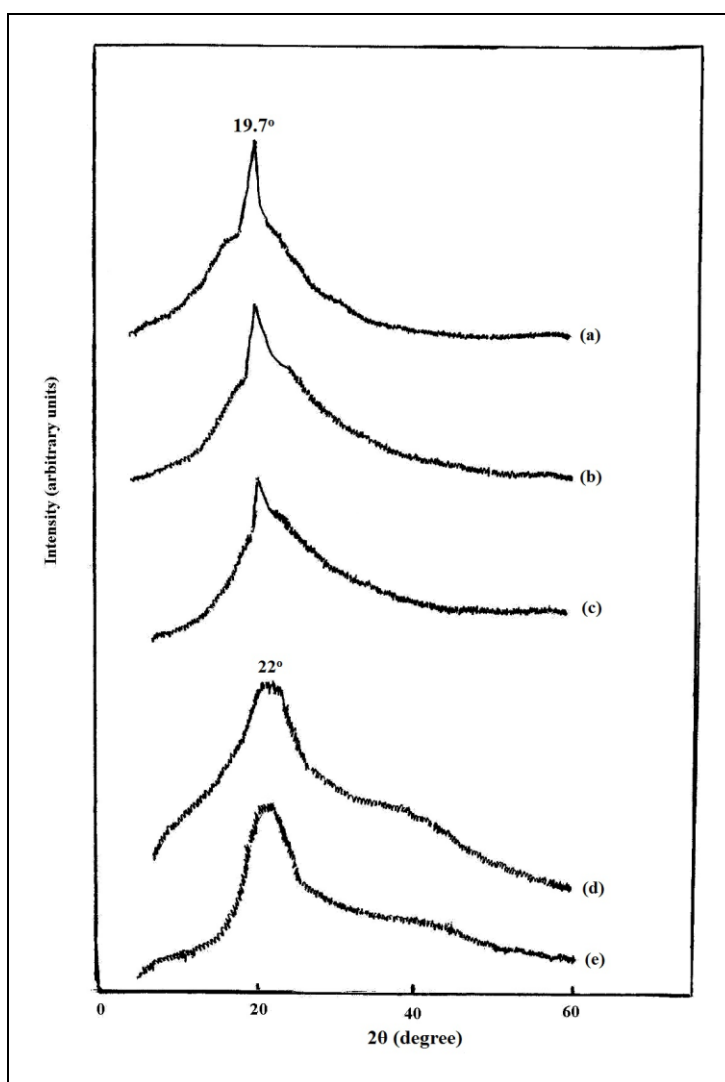


Figure 1. X-ray diffraction patterns for PVA/2HEC blend samples; (a) 100/0, (b) 70/30, (c) 50/50, (d) 30/70 and (e) 0/100 (wt/wt %)

XRD patterns (b and c) of blend samples with concentrations 70 and 50 wt% PVA exhibited the characteristics of pure PVA, but with less intensity for the reflection peak. Thus, one can say that the semi-crystalline structure of PVA is decreased upon mixing with relatively lower content of 2HEC. However, XRD pattern (d) of 30 wt% PVA shows an intense broad halo amorphous covering the positions of those found in homopolymers, for the semi-crystalline/amorphous blends, the non-crystallizing component could strongly modify the crystallization behavior of crystallizing component [16]. For such blends, compatibility between the amorphous components of both homopolymers is possible. Thus, it can be suggested that the crystal forms in PVA do not prevent the compatibility between amorphous regions of the two polymers in the blend system.

3.2. Infrared spectroscopy

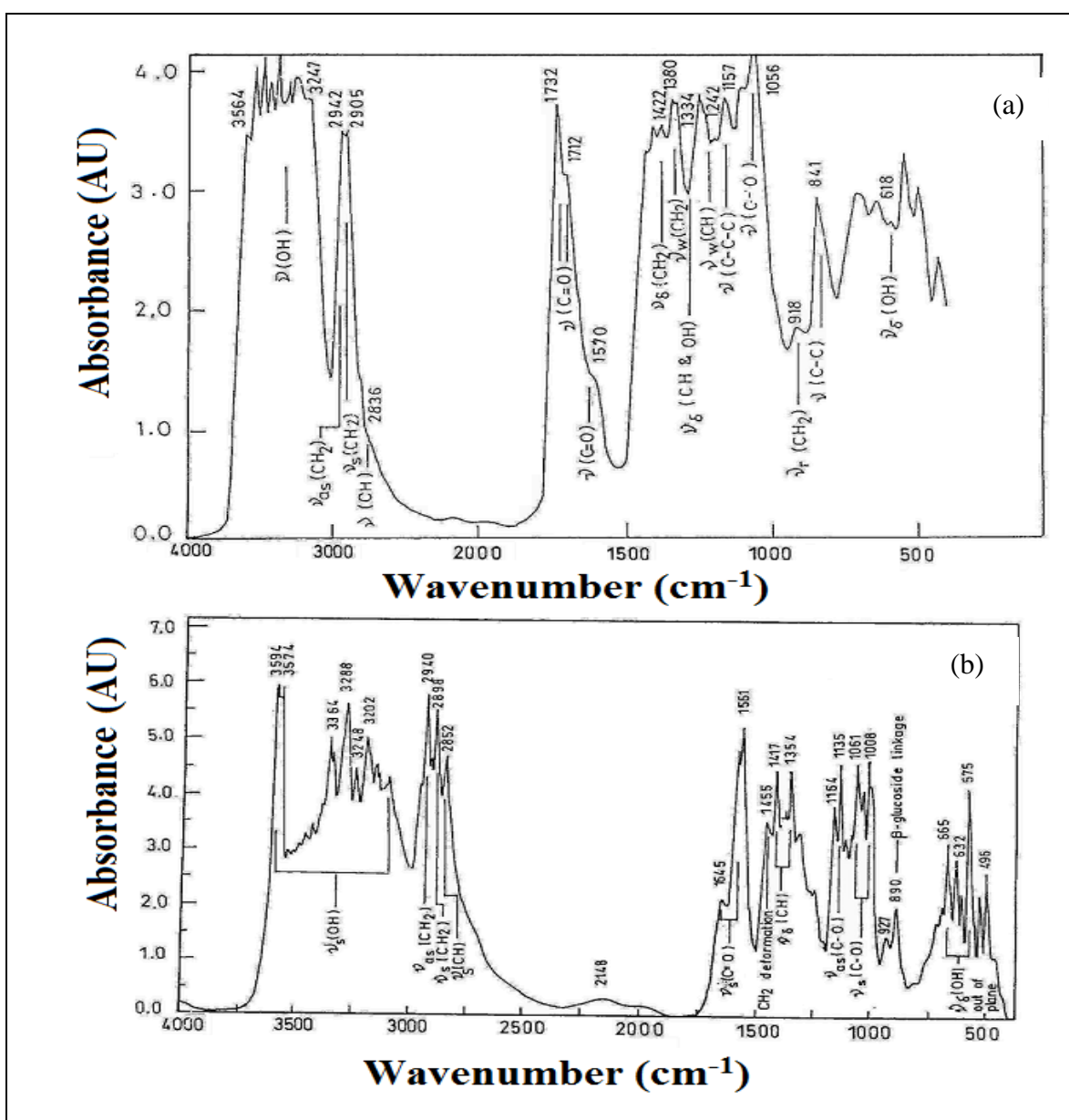


Figure 2. IR spectra of (a) pure PVA and (b) pure 2HEC

Fig. 2 shows the infrared spectra and assignment of the most evident absorption bands for both PVA and 2HEC homopolymers. The spectra (1a) and (1b) of PVA and 2HEC pure polymers respectively are in good agreement with that reported previously [17-23]. Fig. 3 shows the full spectra 4000-400 cm^{-1} of 70/30, 50/50 and 30/70 (wt/wt%) PVA/2HEC blends. Since these two polymers possess some similar functional groups, therefore the group regions of IR spectra are partially the same and their spectra differ only in the fingerprint regions. The blends comprising both compounds show spectra characteristic of both but the vibrational band characterizing each polymer are predominant as its content increases. On the other hand, for frequency region 1500-400 cm^{-1} spectra are so complicated because of the contribution of many different groups that immediate progress in the interpretation of this region seemed doubtful.

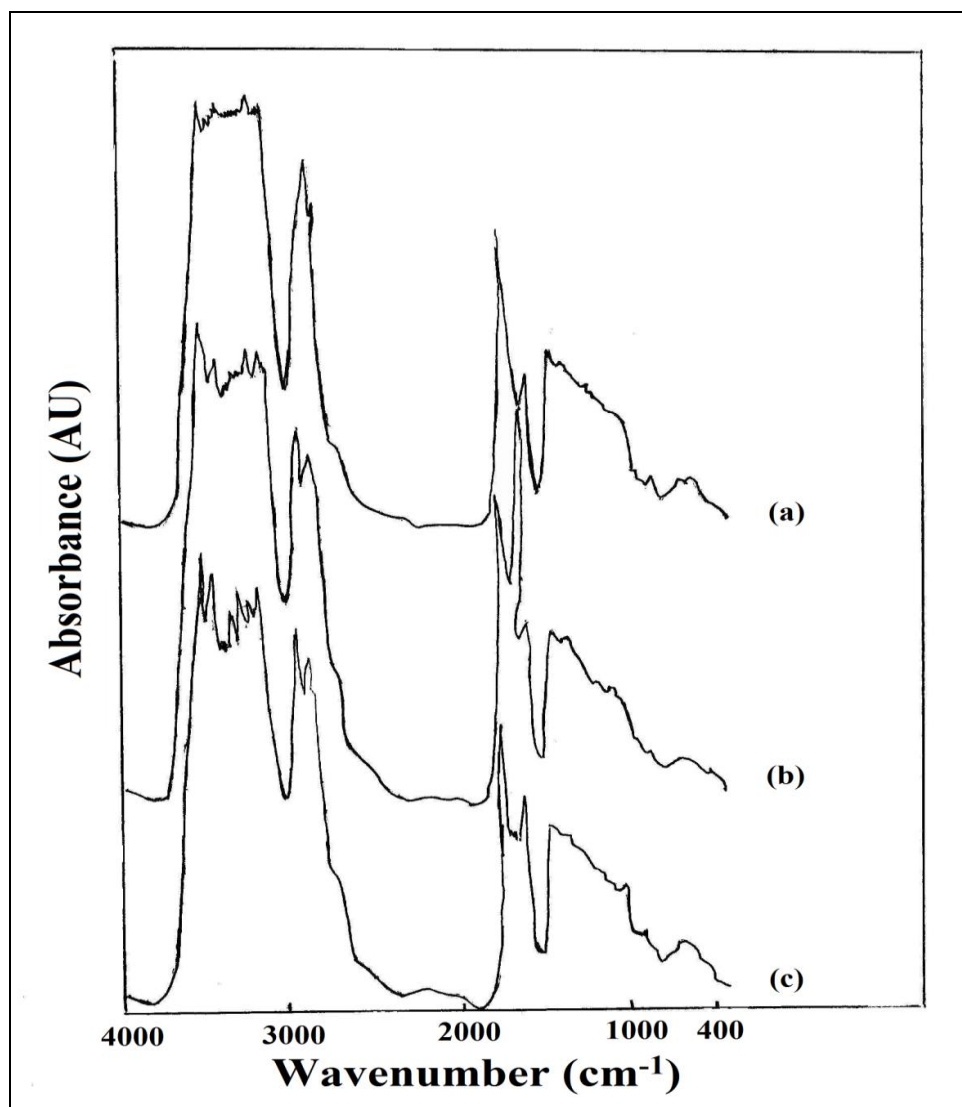


Figure 3. IR spectra of PVA/2HEC blend samples; (a) 70/30, (b) 50/50 and (c) 30/70 (wt/wt %)

The shape of carbonyl bands ($\text{C}=\text{O}$) for blend samples is different from that of pure homopolymers, indicating a change in the balance of free and associated carbonyl groups in the blends. The increase in multiplicity of hydroxyl band (OH) with increasing 2HEC content in blend samples

may reflect possible interactions through hydrogen bonding of hydroxyl beard on the backbone of PVA and 2HEC. In addition the significant deviation of $\nu(C=O)$ at (1732 & 1570) and (1645 & 1561) in pure PVA and 2HEC respectively by about 14, 27, 18 and 36 cm^{-1} , gives an indication to a compatibility between the both polymeric materials in the full composition range.

3.3. UV/visible spectra

The study of optical absorption, particularly the absorption edge has proved to be very useful for elucidation of the optical properties and optical constants of crystalline and non-crystalline materials.

Fig. 4 shows the absorption spectra of PVA and 2HEC homopolymers as well as their blends in the range between 200 and 800 nm. The spectra of pure PVA and pure 2HEC exhibited a shoulder-like band at 280 and 270 nm, respectively which may be due to $\pi \rightarrow \pi^*$ electronic transition (K band) of carbonyl groups. It was reported [4] previously that a relatively strong band at 197 nm associated with the presence of some residual acetate groups appeared in PVA spectrum. This band was not observed in the present work because it is out of range studied.

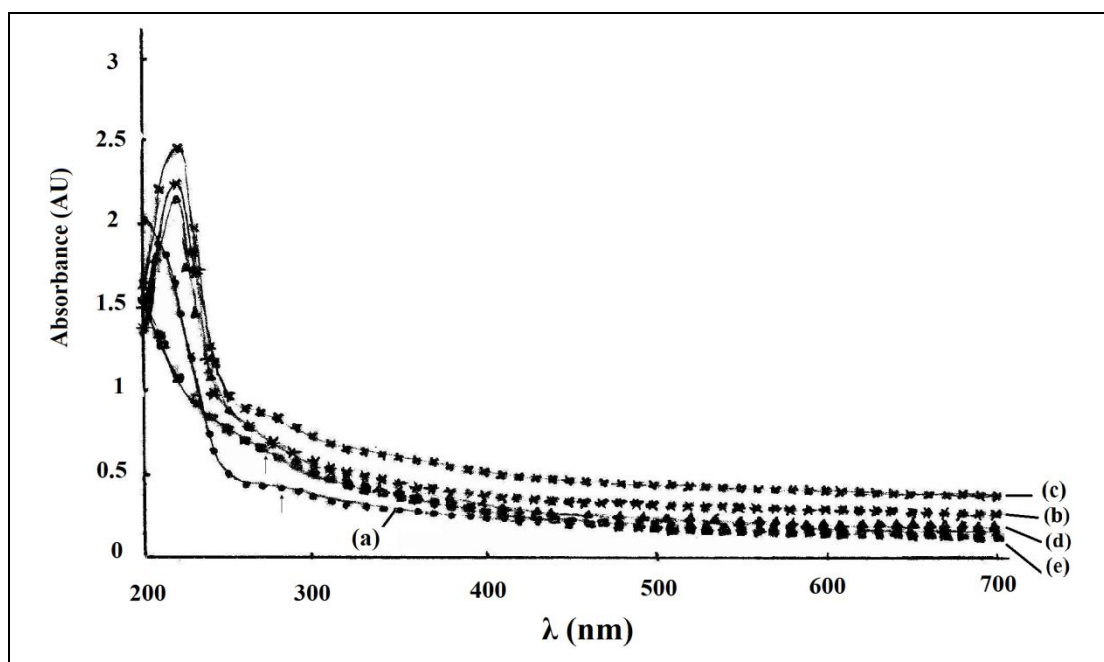


Figure 4. Absorbance spectra of PVA/2HEC blend samples; (a) 100/0, (b) 70/30, (c) 50/50, (d) 30/70 and (e) 0/100 (wt/wt %)

The UV/visible spectra for the blended PVA/2HEC samples with compositions of 70/30, 50/50 and 30/70 (wt/wt %) contained a sharp intense band at 225 nm beside the shoulder-like band at about 275 nm. Thus, the addition 2HEC to PVA shifted the band at 197 nm in pure PVA toward higher wavelengths by about 28 nm.

The absorption coefficient (α) was calculated from the absorbance (A) using the relation:

$$\alpha = \frac{2.303}{x} A \tag{1}$$

where x is the thickness of the sample. The values of α for the samples under investigation are relatively small ($50\text{-}1200\text{ cm}^{-1}$) indicating that the materials are weakly absorbing. Fig. 5 shows the dependence of the absorption coefficient (α) on photon energy ($h\nu$) for PVA and 2HEC homopolymers and their blended samples. The $\alpha(\nu)$ exhibits a steep rise near the absorption edge and then rapidly increases in a straight line relationship in the relatively high α -region. The rapid increase of absorption coefficient is attributed to interband transitions. The intercept of extrapolation to zero absorption with photon energy axis was taken as the value of absorption edge. The data are presented in Table 1. It is clear that the values of absorption edge for blend samples are in between for individual polymers and decrease with decreasing the PVA content. This may reflect the induced changes in the number of available final states according to blend compositions.

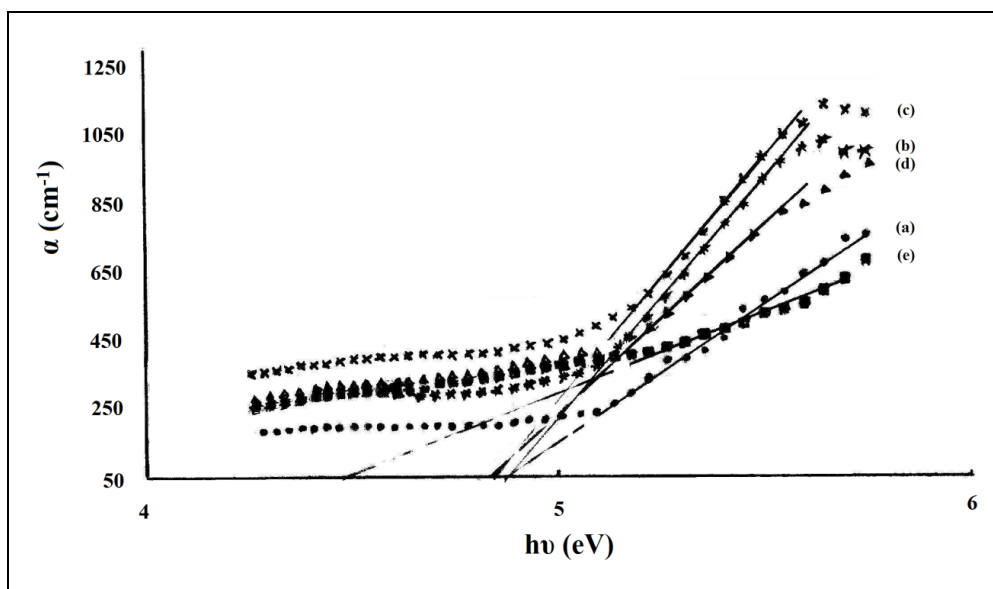


Figure 5. Absorbance coefficient (α) as a function of photon energy ($h\nu$) for PVA/2HEC blend samples; (a) 100/0, (b) 70/30, (c) 50/50, (d) 30/70 and (e) 0/100 (wt/wt %)

Table 1. values of absorption edge, energy tail and refractive index of PVA and 2HEC homopolymers and their blend samples.

PVA/2HEC (wt/wt %)	Absorption edge (eV)	Energy tail (eV)	Refractive index (n_o)
100/0	4.86	1.00	1.68
70/30	4.85	0.80	1.55
50/50	4.83	0.66	1.63
30/70	4.80	0.68	1.65
0/100	4.47	1.08	1.53

In the exponent edge where the absorption coefficient, $1 < \alpha < 10^4 \text{ cm}^{-1}$, is governed by an empirical relation due to Urbach [24],

$$\alpha = \alpha_o \exp\left(\frac{h\nu}{E_e}\right) \tag{2}$$

where α_o is a constant and E_e is the width of the band tails of the localized states in the films. Fig. 6 shows the relation between $\ln(\alpha)$ and $h\nu$ for PVA and 2HEC homopolymers as well as their blends. The straight lines obtained suggest that the absorption follows the quadratic relation for interband transition [25] and obey the Urbach rule. The values of band tail E_e were calculated from the reciprocal of the slopes of these lines and are listed in Table 1. The values of E_e obtained for blend samples are varying slightly with composition. Thus, it can be suggested that the formation of blended samples probably induce tails in the density of states by perturbing the band edge via a deformation potential, coulomb interaction and by forming localized band states [26].

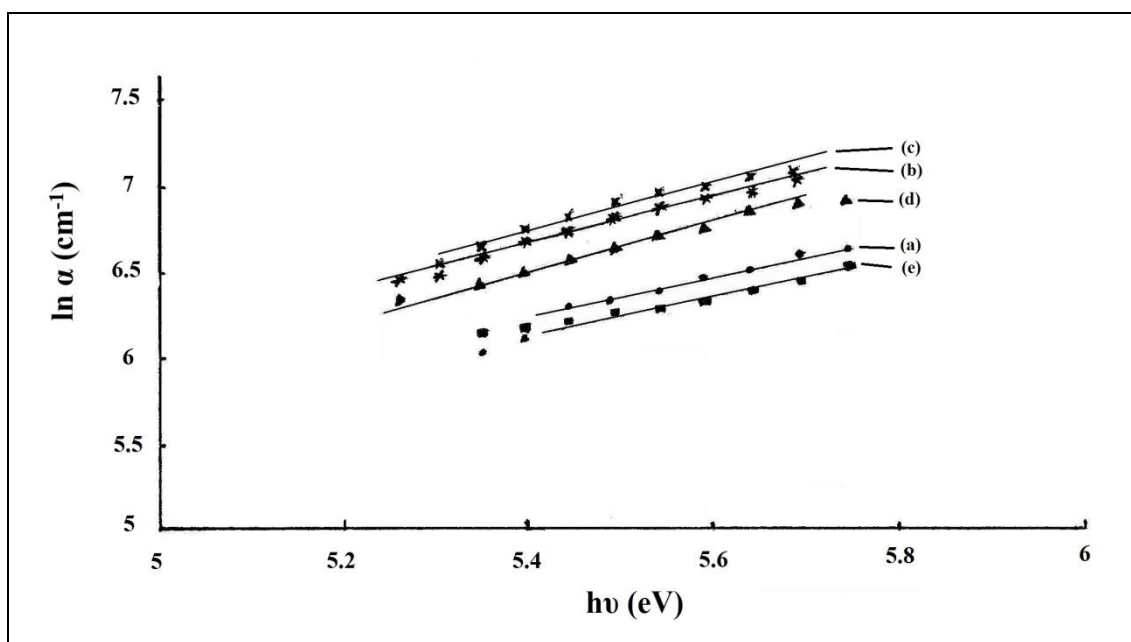


Figure 6. Relation between $\ln(\alpha)$ and $(h\nu)$ for PVA/2HEC blend samples; (a) 100/0, (b) 70/30, (c) 50/50, (d) 30/70 and (e) 0/100 (wt/wt %)

The reflectance (R), the extinction coefficient (K) and the refractive index (n) of the samples are related through the following two equations:

$$K = \frac{\alpha\lambda}{4\pi} \tag{3}$$

$$R = \frac{(n-1)^2 + K^2}{(n+1)^2 + K^2} \tag{4}$$

Relation (4) was used to calculate n from measurement of absorbance and reflectance (Figure

not shown for sake of brevity). The values of K for all samples are found small in the range $(10^{-4} - 10^{-3})$ indicating that the investigated samples are insulators without any defects [27]. Fig. 7 shows the $n(\lambda)$ spectra from 400 to 800 nm at room temperature for all investigated samples. It is clear from the figure that the refractive index increases slightly with decreasing wavelength and the changes become larger at shorter wavelengths showing the typical shape of a dispersion curve. The nearly constant values of refractive indices at longer wavelengths (n_o) are listed in Table 1. It must be mentioned that the values of refractive index of blend samples lie in between the values of homopolymers. Also, the refractive index of blend samples increased with increasing the 2HEC concentrations. The compositional dependence of refractive index can be caused by the interference phenomena due to the domain structure, molecular orientation and processing conditions [28]. The relatively high values of refractive index may be attributed to an increase in the valence density of charge carriers in the present samples.

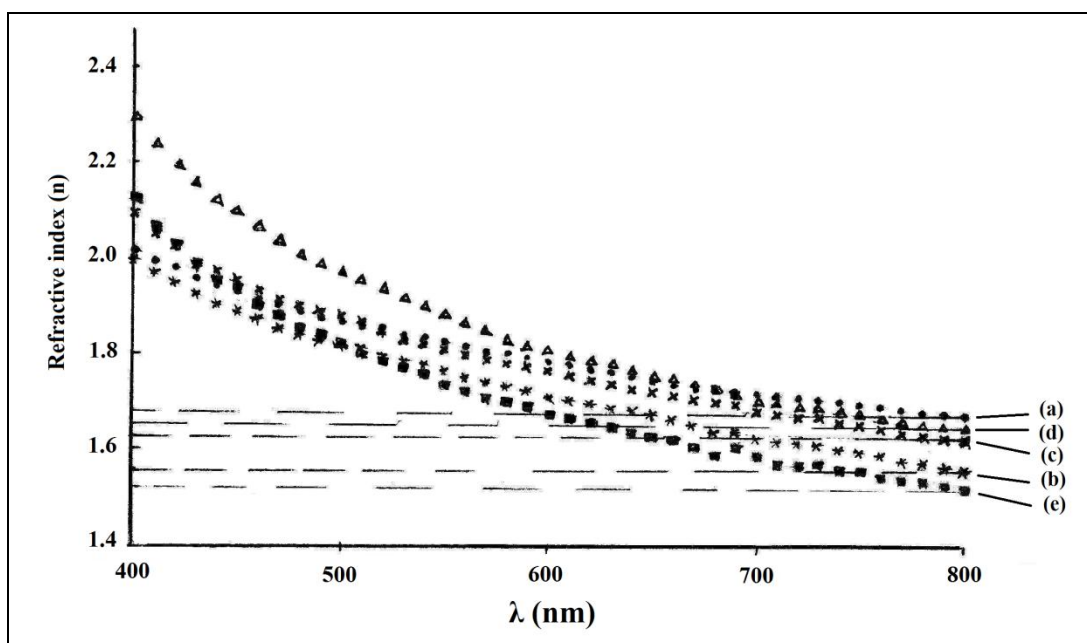


Figure 7. Variation in refractive index with wavelength for PVA/2HEC blend samples; (a) 100/0, (b) 70/30, (c) 50/50, (d) 30/70 and (e) 0/100 (wt/wt %)

3.4. Thermal analysis.

3.4.1 Differential thermal analyses.

The presence of water as a solvent could modify self-association of both PVA and 2HEC and interaction between components in the blend samples. These polymers are heat-sensitive; after thermal treatment their absorption capacity for the water are modified. Therefore, the samples under investigation were annealed at 100 °C for 15 minutes for complete evaporation of water solvent before any studies.

Fig. 8 shows the DTA thermographs of all samples in the temperature range from 30 up to 400 °C. The glass transition temperatures (T_g) and melting points (T_m) of PVA and 2HEC are in close agreement with those reported in literature [29-32]. The small deviation of T_g values for both individual polymers from that previously reported might be due to the difference in purity, processing conditions, rate of heating and/or the instrument employed. Glass transition temperature, melting point and decomposition temperature are reported in Table 2. It must be noted that the T_g value of the blend samples and melting point of PVA in such system decrease with increasing 2HEC concentrations. On the other hand, the melting transition of 2HEC and the decomposition temperature (T_d) of PVA in blend samples increase with increasing PVA concentrations. It seems that the intermolecular interaction between PVA and 2HEC can strengthen the molecular backbones of 2HEC which may be a direct result of its rigid nature. This results support that PVA/2HEC blends have certain miscibility level in the amorphous state.

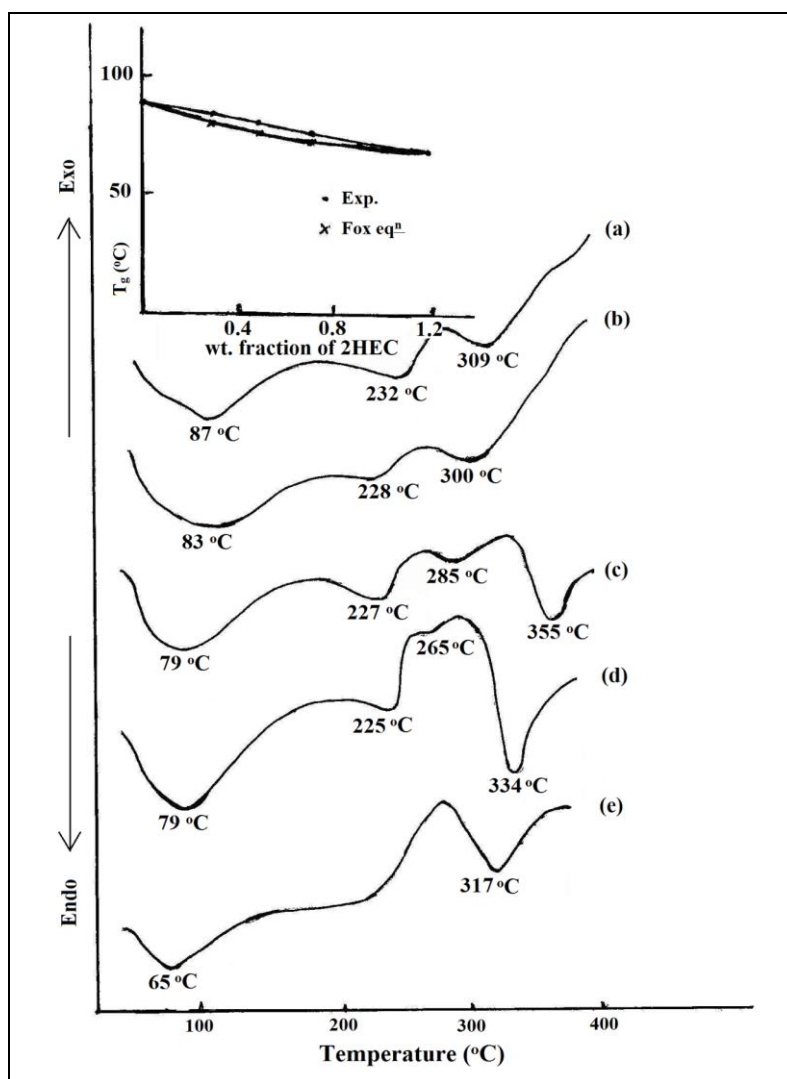


Figure 8. DTA thermograms for PVA/2HEC blend samples; (a) 100/0, (b) 70/30, (c) 50/50, (d) 30/70 and (e) 0/100 (wt/wt %)

Table 2. Transition temperature for PVA/2HEC (wt/wt%) blend samples.

PVA/2HEC (wt/wt%)	Glass transition temperature	Melting phase transition T_m		Dissociation temperature
	T_g °C	PVA	2HEC	T_D °C
100/0	87	232	----	309
70/30	83	228	NT	300
50/50	79	227	355	285
30/70	74	225	334	265
0/100	65	----	317	----

---- Not detected; may be due to the little amount of 2HEC or out of the measured temperature range.

There are several classical equations that correlate the glass transition temperature of miscible blend system with its composition [33-36]. Fox equation [33] is given by

$$\frac{1}{T_{g(\text{blend})}} = \frac{w_1}{T_{g_1}} + \frac{w_2}{T_{g_2}} \quad (5)$$

where w_1 and w_2 are the weight fractions; T_{g_1} and T_{g_2} are the respective glass transition temperatures of the homopolymers. The glass transition temperatures estimated using Fox equation and T_g from the DTA curves (experimental) for the studied blends as a function of 2HEC content are shown in the inset of Fig.8. It is apparent from the inset of Fig. 8 that the experimental data of T_g for the blends do not follow the calculated theoretical values by Fox rule quite well, the deviation are in the range 5 up to 7 %. For all systems, the experimental T_g values are somewhat higher than ideal values exhibiting positive deviation. This may allow one to consider the possibility of a relatively strong compatibility between PVA and 2HEC in the full composition range.

3.4.2 Thermogravimetric analysis.

TGA is widely used to investigate the thermal decomposition of polymers and to determine the kinetic parameters such as activation energy (E), enthalpy (ΔH), entropy (ΔS) and Gibbs free energy (ΔG), these parameters can be used to give a better understanding of the thermal properties of polymer blends.

From the thermograms in Fig. 9, it can be seen that all samples present three stages in the mass loss curve. These stages are distinguishable in the diagram of mass loss (TG %) during heating as well as -more clearly- in the diagram of derivative mass loss (D_rTG). Table 3 represents the decomposition steps and percentage weight loss for individual polymers and their blends. The lower values of percentage weight loss in the first decomposition step are attributed to the volatilization of small molecules and/or evaporation of residual absorbed water. The percentage weight loss in the second decomposition step, which included both melting point and the degradation temperature of PVA, is

attributed to splitting of monomers and bond scission in the polymeric backbone. The major percentage weight loss in the third decomposition step is attributed to fragmentation of the macromolecular structure for both PVA and 2HEC polymers.

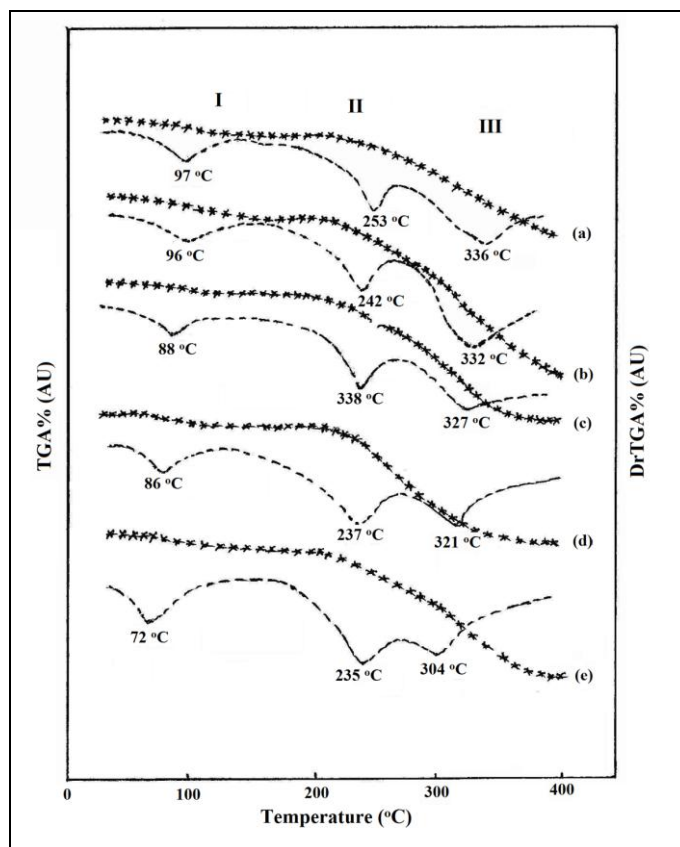


Figure 9. TG and DrTG of PVA/2HEC blend samples; (a) 100/0, (b) 70/30, (c) 50/50, (d) 30/70 and (e) 0/100 (wt/wt %)

Table 3. TG and Dr TG data for PVA/2HEC (wt/wt%) blend samples.

PVA/2HEC (wt/wt%)	Temperature °C			% weight loss	
	Start	End	T_p^*	Partial	Total
100/0	44	153	97	7.46	62.09
	153	273	253	15.96	
	273	400	336	36.73	
70/30	50	164	96	7.46	62.73
	183	273	242	13.43	
	273	400	332	41.03	
50/50	36	177	88	6.97	69.00
	177	253	238	13.66	
	253	400	327	48.43	
30/70	35	171	86	6.21	71.10
	171	256	237	15.97	
	256	400	321	48.92	
0/100	41	161	72	6.69	74.61
	162	271	235	28.81	
	271	400	304	38.58	

T_p^* : peak temperature of Dr TG.

The peak temperature (T_p) of D_rTG and the total weight loss are used as a measure of thermal stability. Thus, the curves show that thermal stability of the blend samples lies in between those of the homopolymers. The thermal stability of blend samples is enhanced by increasing the PVA content.

It is to be noted that the peak temperatures T_p of D_rTG curves in decomposition regions for blend samples are shifted to higher temperatures compared to pure 2HEC with the increase of PVA concentrations but still less than pure PVA. Thus, the higher thermal stability of blend samples compared to pure 2HEC could be attributed to the intermolecular crosslinking reaction, which gives highly compatible impact blend polymers. In addition, the sample composition 70/30 (wt/wt %) PVA/2HEC exhibits a high bonding strength in this system due to crosslink formation, since a little amount of total weight loss is recorded. This stability enhances the use of 2HEC for commercial applications for item production via melt processing techniques.

In order to be analyzed more deeply the degradation mechanisms of present samples, it is important that the kinetic parameters be evaluated by making use of the well known Coats-Redfern [37] relation:

$$\ln \left[\frac{-\ln(1-\delta)}{T^2} \right] = \frac{-E}{RT} + \frac{AR}{\beta E} \quad (6)$$

where A is a constant, β is the heating rate, R is the universal gas constant, E is the activation energy and δ is the fractional weight loss. The plots of $\ln \left[\frac{-\ln(1-\delta)}{T^2} \right]$ against $\frac{1}{T}$ for individual polymers and their blend samples in the first decomposition region gives a straight line and the slope of these lines gives the activation energy $\left(\frac{-E}{R} \right)$. The thermodynamic parameters ΔS , ΔH and ΔG were calculated using the following equations:

$$\Delta S = 2.303R \left(\log \frac{Ah}{K_B T} \right) \quad (7)$$

$$\Delta H = E - RT \quad (8)$$

$$\Delta G = \Delta H - T \Delta S \quad (9)$$

where K_B and h are Boltzmann and Planck constants, respectively, T is the temperature at the end of decomposition step. Fig. 10 represents the Coats-Redfern plots of the first decomposition step for individual polymers and their blend samples. An obtained value of about 0.987 for R^2 (correlation coefficient) indicates a good correlation for the decomposition step. The calculated thermodynamic parameters values are given in Table 4. The activation energies for pure polymers as well as their blends are relatively small at the initial stage of degradation. These initial lower values are likely associated with initiation process that occurs at weak links of PVA and 2HEC which is, however, a limited step of degradation. It is clear that the values of E and ΔH for blend samples of 70 and 30 wt%

PVA content are lower than those for the homopolymers while the values of the blend samples of 50 wt% PVA content is the higher one. In addition, the values of ΔS for blend samples change irregularly with compositions, while ΔG values lie nearly in the same order of individual polymers. Moreover, all samples have negative entropy that indicates ordered systems and more ordered activated states that may be possible through the chemisorption of other light decomposition products. Therefore, it can be concluded that the blend sample of 50/50 (wt/wt%) has more thermal motion and lower order than the other samples.

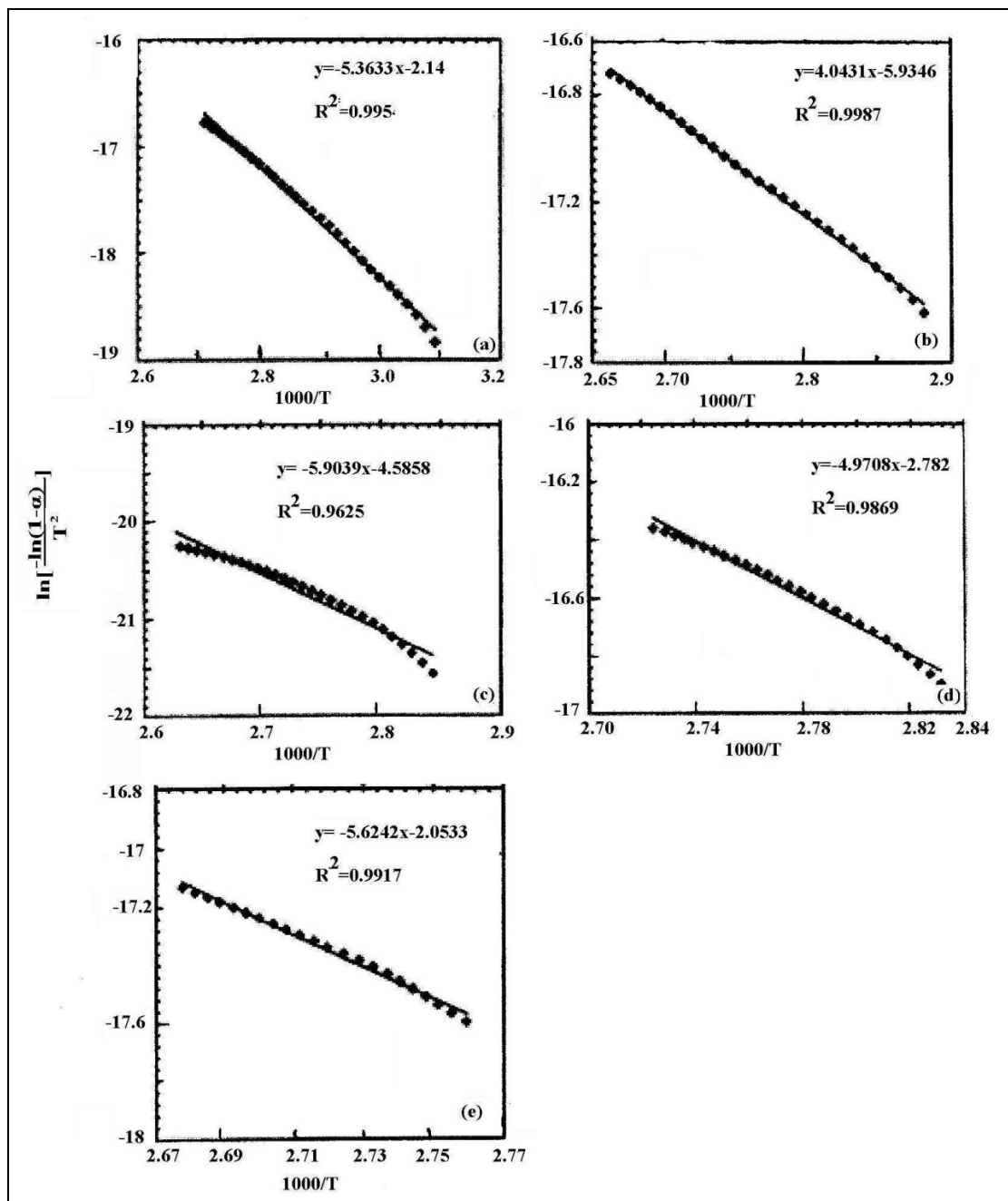


Figure 10. Coats-Redfern plots of the first decomposition step for PVA/2HEC blend samples; (a) 100/0, (b) 70/30, (c) 50/50, (d) 30/70 and (e) 0/100 (wt/wt %)

Table 4. Thermodynamic parameters for PVA/2HEC (wt/wt%) blend samples in the first decomposition step.

PVA/2HEC (wt/wt%)	E KJ/gm. mole	ΔS J/K. mole	ΔH KJ/mole	ΔG KJ/mole
100/0	44.6	-68.8	41.5	67.4
70/30	33.6	-103.1	30.5	68.9
50/50	49.1	-59.2	46.1	67.6
30/70	41.3	-77.5	38.4	65.5
0/100	46.8	-64.3	43.7	67.2

4. CONCLUSIONS

(i) X-ray diffraction of the blend samples of 30 and 50 wt% 2HEC content revealed that the semi-crystalline structure of PVA is essentially sustained while for relatively higher concentration 70 wt% the halo amorphous is observed only as a broader one.

(ii) On the basis of the observed data from XRD, IR spectroscopy and differential thermal analyses, it could be concluded that the formation of hydrogen-bonding between PVA and 2HEC is possible within the investigated composition ranges.

(iii) The analysis of absorption coefficient data reflects the long band tails of width in the range 0.66 up to 1.08 eV. Optical absorption edges showed a decreasing trend with increasing 2HEC concentrations in blend samples, while the refractive index has an opposite behavior.

(iv) The activation energy calculated by using Coast-Redfern relation in first decomposition step is the highest for 50 wt% PVA sample which indicates that this blend is relatively harder and highly compatible impact due to intermolecular crosslinking reaction.

References

1. N. Reddeppa, T. J. R. Reddy, V. B. S. Achari, V. V. R. Rao and A. K. Sharma, *Ionics*, 15 (2009) 255
2. F. H. Abd El-Kader, S. A. Gafer, A. F. Basha, S. I. Bannan and M. A. F. Basha, *J. Appl. Polym. Sci.*, 118 (2010) 413
3. M. H. Buraidah and A. K. Arof, *J. Non-crystalline Solids*, 357 (2011) 3261
4. N. Limpan, T. Prodpran, S. Benjakul and S. Prasarpran, *Food Hydrocolloids*, 29 (2012) 226
5. C. H. Cholakis, W. Zingg, M. V. Sefton, *J. Biomed. Mater. Res.*, 23 (1989) 417
6. D. R. Garrel, P. Gaudreau, L. M. Zhang, I. Reeves and P. Brazeau, *J. Surg. Res.*, 51 (1991) 297
7. S. Horiike and S. Matsuzawa, *J. Appl. Polym. Sci.*, 58 (1995) 1335
8. G. Paradossi, F. Covalieri, E. Chiessi, C. Spagnoli and M. K. Cowman, *J. Mater. Sci. Mater Med.*, 14 (2003) 687
9. M. Zhai, F. Yoshii and T. Kume, *Carbohydrate Polymes*, 52 (2003) 311
10. B. Ramaraj, *J. Appl. Polym. Sci.*, 103 (2007) 909
11. M. T. Clarke, CIE-Conference, *Wiesbaden Germany* (1990).
12. L. G. Patruyo, A. J. Muller and A. E. Saez, *Polymer*, 43 (2002) 6481
13. J. Hedin, A. Ostlund and M. Nyden, *Carbohydrate Polymer*, 79 (2010) 606

14. H. N. Friedlander, H. E. Harris and J. G. Pritchard, *J. Polym. Sci. part A-1: Polymer chemistry*, 4 (2003) 649
15. G. D. Wignall, Scattering Techniques, in physical properties of polymers, American chemical Society, Washington DC (1993)
16. Y. W. Cheung and M. J. Guest, *J. Polym. Sci. Part B: Polym. Phys.*, 38 (2000) 2976
17. J. R. Fried, *Polymer science and Technology*, Prentice Hall, New Jersey (1995)
18. J. G. Pritchard, *Poly(vinyl alcohol); basic properties and uses*, Gordon and Breach, New York (1970)
19. C. J. Creswell, O. A. Runquist and M. M. Campbell, *Spectral Analysis of Organic Compounds*, Burgess Publishing Company, USA (1972)
20. D. L. Pavia, G. M. Lampman and G. S. Kriz, *Introduction to Spectroscopy*, W. B. Saunders, Philadelphia (1979)
21. B. G. Osborne and T. Fearn, *Near Infrared Spectroscopy in Food Analysis*, Longman Scientific & Technical; U. K. (1986)
22. J. Li, J. F. Revol and R. H. Marchessault, *J. Appl. Polym. Sci.*, 65 (1997) 373
23. F. H. Abd El-Kader, S. A. Gafer, H. S. Rizk and N. A. Kamel, *J. Appl. Polym. Sci.*, 72 (1999) 1395
24. F. Urboch, *Phys. Rev.*, 92 (1953) 1324
25. E. A. Davis and N. F. Mott, *Philos. Mag.*, 22 (1970) 903
26. N. F. Mott and E. A. Davis, *Electronic processes in Non-crystalline Materials*, Clarendon Press, Oxford; Oxford University Press, New York (1979)
27. J. I. Pankove, *Optical Processes in Semiconductors*, Dover Publication, New York (1975)
28. H. Y. Joo, H. J. Kim, S. J. Kim and S. Y. Kim, *J. Vac. Sci. Technol. A*, 17 (1999) 862
29. D. Marianiova, L. Lapcik and M. Pisarcik, *Acta Polymerica*, 43 (1992) 303
30. S. K. Mallapragada and N. A. Peppas, *J. Polym. Sci. Part B: Polym. Phys.*, 34 (1996) 1339
31. Y. Kong and J. N. Hay, *Polymer*, 43 (2002) 3873
32. F. H. Abd El-kader, A. M. Shehap, M. S. Abo-Ellil and K. H. Mahmoud, *J. Poly. Mater.*, 22 (2005) 349
33. T. G. Fox, *Bull. Am. Phys. Soc.*, 1 (1956) 123
34. M. Gordon and J. S. Taylor, *J. Appl. Chem.*, 2 (1952) 495
35. T. K. Kwei, *J. Polym. Sci. Polym. Lett. Edn.*, 22 (1984) 307
36. H. K. Kim and F. G. Shi, *J. Mater. Sci. Mater. Electron.*, 12 (2001) 361
37. A. W. Coats, J. P. Redfern, *Nature*, 201 (1964) 68